# Frequency Dependent X-Ray Fluences from a High Yield Light Ion Beam Fusion Target Explosion in a Gas Filled Chamber

G.A. Moses

September 1982

UWFDM-486

FUSION TECHNOLOGY INSTITUTE

UNIVERSITY OF WISCONSIN

MADISON WISCONSIN

# Frequency Dependent X-Ray Fluences from a High Yield Light Ion Beam Fusion Target Explosion in a Gas Filled Chamber

G.A. Moses

Fusion Technology Institute
University of Wisconsin
1500 Engineering Drive
Madison, WI 53706

http://fti.neep.wisc.edu

September 1982

UWFDM-486

# FREQUENCY DEPENDENT X-RAY FLUENCES FROM A HIGH YIELD LIGHT ION BEAM FUSION TARGET EXPLOSION IN A GAS FILLED CHAMBER

G.A. Moses

Fusion Engineering Program
Nuclear Engineering Department
University of Wisconsin-Madison
Madison, Wisconsin 53706

September 1982

UWFDM-486

Abstract

Multifrequency x-ray fluences are calculated for a particular high yield light ion beam fusion target. The prompt x-rays from the target are partially attenuated by the gas filled chamber. This gas then re-radiates the absorbed energy to the wall in a much softer spectrum. These calculations are done for two chamber gases (10 torr of argon and nitrogen) and for two positions from the target (1 and 3 meters).

## I. Introduction

The light ion fusion target development facility (TDF)[1] has been designed for the purpose of developing and testing high yield targets. These targets are expected to give yields in the range of 50 to 200 MJ with an input energy of 4-8 MJ of light ions. The reaction chamber that contains these ~ 100 MJ explosions is 3 meters in radius and is filled with ~ 10 torr of gas such as argon or nitrogen. This gas is necessary to support the formation of z-pinch plasma channels to allow propagation of the ion beams from individual diodes behind the chamber first wall to the target.[2] The exploding target releases about 70% of its thermonuclear energy in the form of high energy neutrons and gamma rays. The remainder of the energy is in the form of x-rays and expanding ions. This energy is partially attenuated or stopped by the chamber gas, resulting in the formation of a fireball. This fireball propagates to the first wall and subjects it to a surface heat flux and overpressure.[3-5]

Any diagnostic packages at the first wall or internal to the first wall will be exposed to at least 4 forms of electromagnetic radiation:

1. Prompt target gamma rays.
2. Prompt target x-rays.
3. Fireball thermal x-rays.
4. EMP.

In this report we investigate the first three of these forms for a particular light ion fusion target design.[6] We look at the problem for two types of chamber gas: (1) 10 torr of argon, and (2) 10 torr of nitrogen. We also compute the frequency dependent x-ray energy fluence at two distances from the target: (1) 1 meter, and (2) 3 meters. A schematic picture of this problem is shown in Fig. 1.

## II. Light Ion Fusion Target

The light ion fusion target used in this study was originally designed and reported by Bangerter.[6] It was slightly modified during the HIBALL study[7] and the modified target is shown in Fig. 2. In this diagram we show the target in its initial configuration and also in its configuration at the time of ignition. This ignition state was estimated from the reported yield of 113 MJ. Using this final configuration as our initial condition we simulated the thermonuclear burning of the fuel and the hydrodynamic disassembly of the target using the PHD-IV hydrodynamics-thermonuclear burn-radiative transfer computer code.[8] We also did an independent neutron transport calculation for this compressed target using the ANISN code[9] to estimate the spectrum of neutrons and gamma rays escaping from the target. These hydrodynamic and transport calculations were reported elsewhere.[7,10] Using these two calculations we estimate the energy partitioning of the target to be that shown in Table 1. The results are normalized to a yield of exactly 100 MJ for convenience. This represents only a 13% adjustment of the results and is certainly well within the accuracy of these calculations. The neutron spectrum from the target is shown in Fig. 3 and the gamma ray spectrum is shown in Fig. 4. The x-ray spectrum is shown in Fig. 5. The partitioning of the ion energy between the different species is given in Table 2. These results now serve as input to the fireball calculations discussed in the next section.

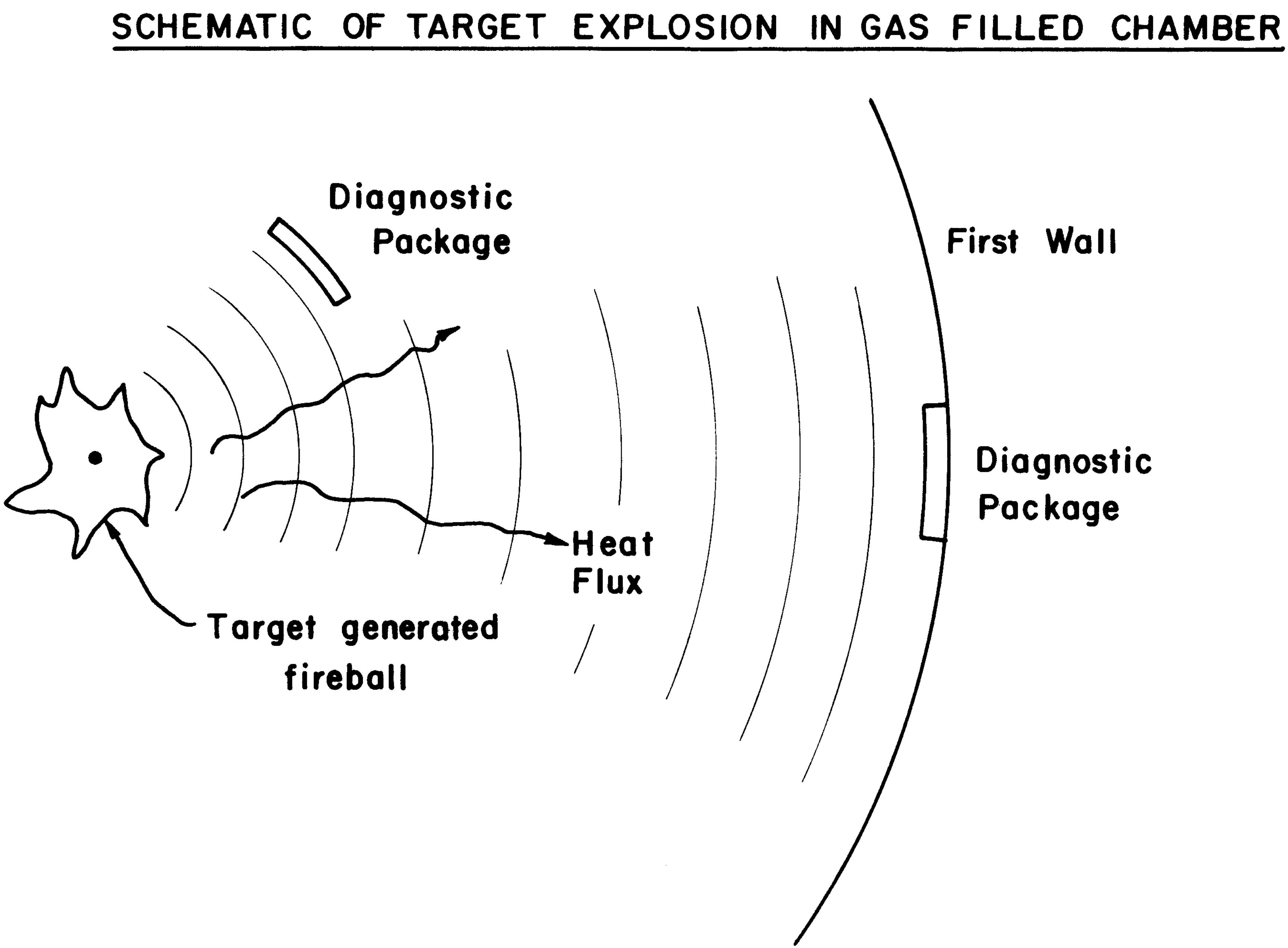


Figure 1 Schematic of target explosion in TDF reaction chamber.

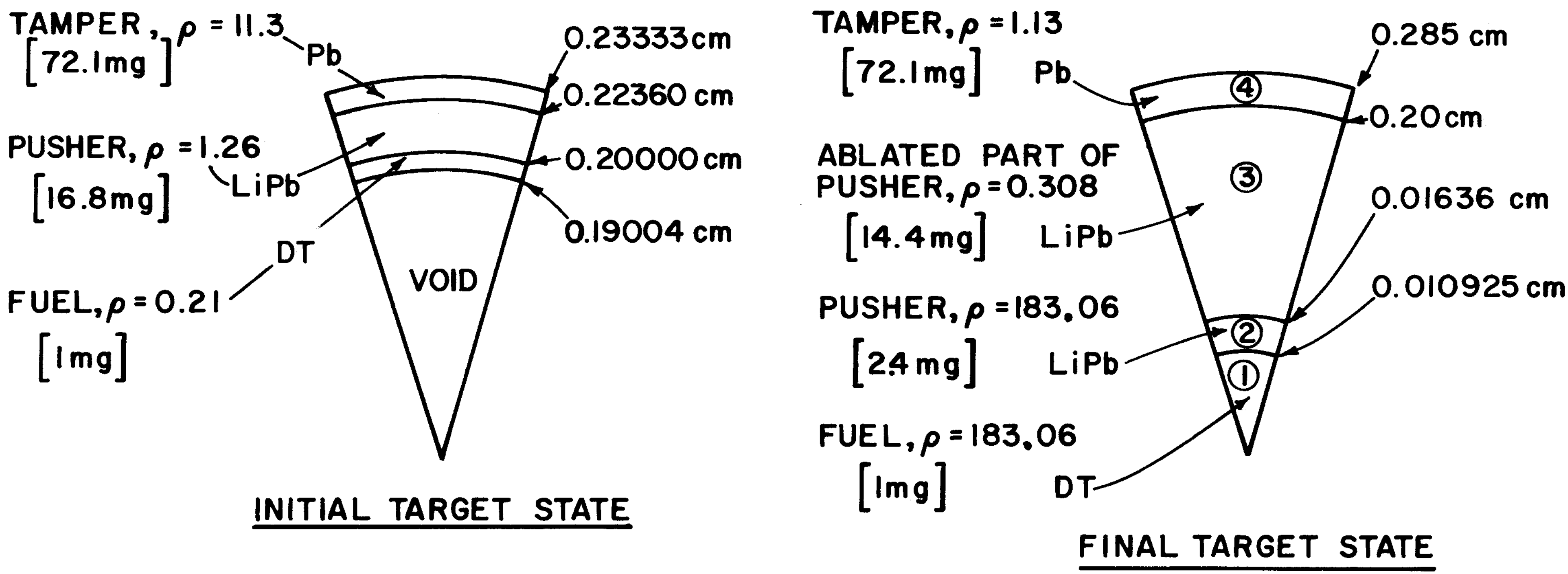


Figure 2 Light ion fusion target.

Table 1. Energy Partitioning of the Light Ion Fusion Target

| | |
|---|---|
| Neutrons | 70.75 MJ |
| $\gamma$-rays | 0.15 MJ |
| X-rays | 23 MJ |
| Ion Debris | 5.1 MJ |
| Endothermic | 1 MJ |
| | 100 MJ |

Table 2. Partitioning of Energy Between Ion Species

| Species | Energy/Ion | Energy/Species |
|---|---|---|
| D | 1.2 keV/ion | 0.016 MJ |
| T | 1.76 keV/ion | 0.024 MJ |
| $He^4$ | 2.34 keV/ion | 0.013 MJ |
| Li | 4.1 keV/ion | 0.38 MJ |
| Pb | 121. keV/ion | 4.63 MJ |
| | | 5.1 MJ |

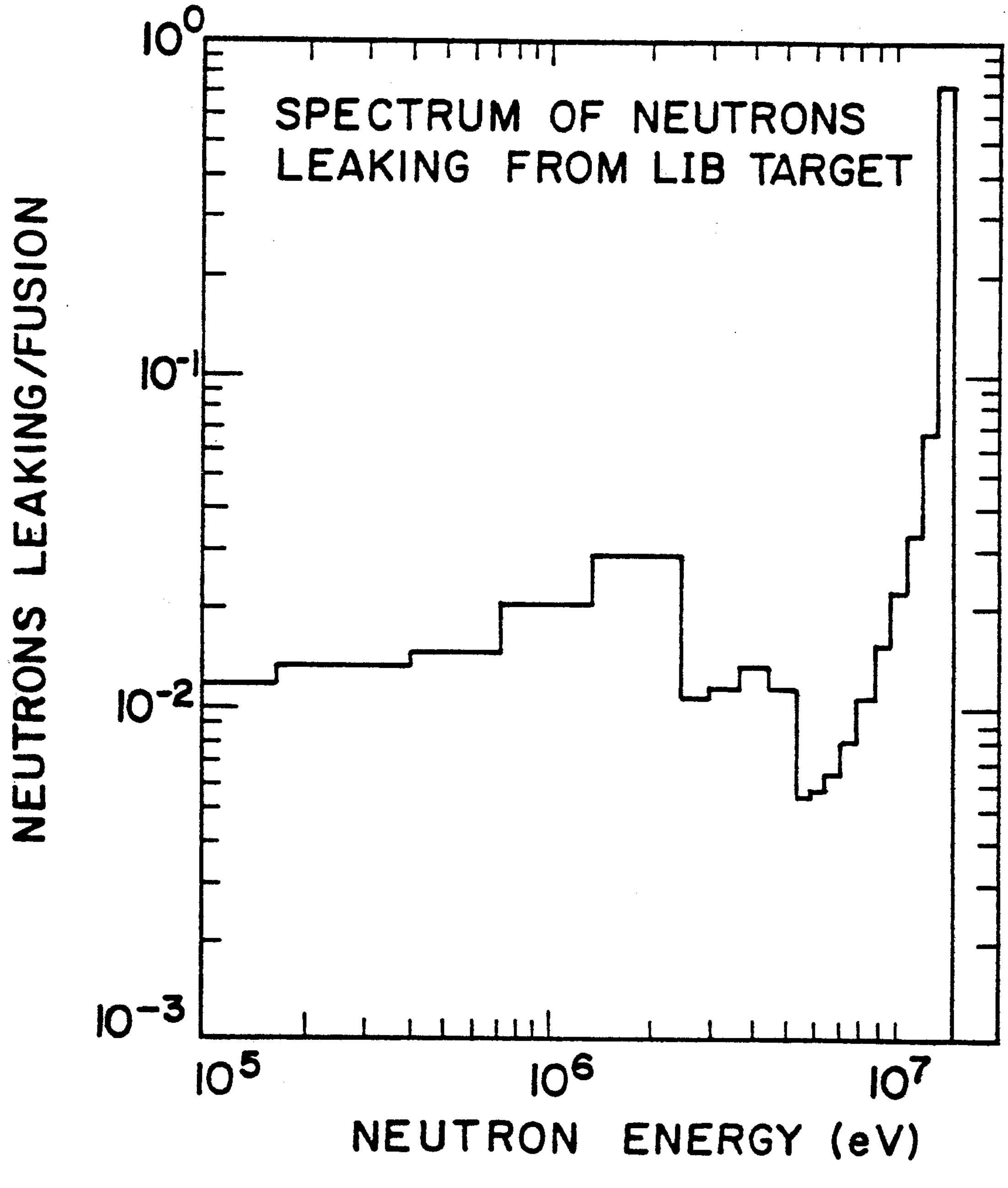


Figure 3  Neutron spectrum of light ion fusion target.

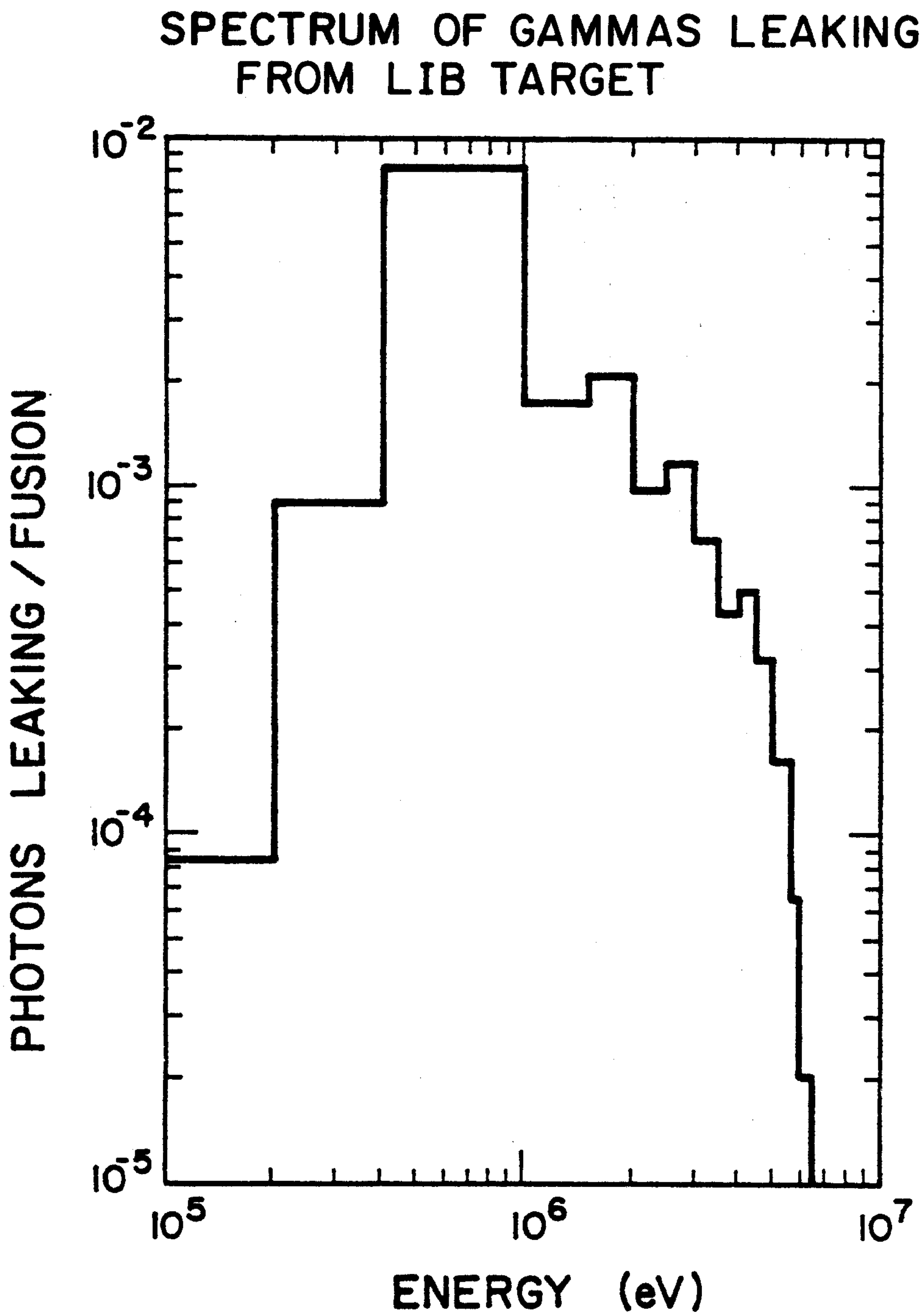


Figure 4 Gamma ray spectrum of light ion fusion target.

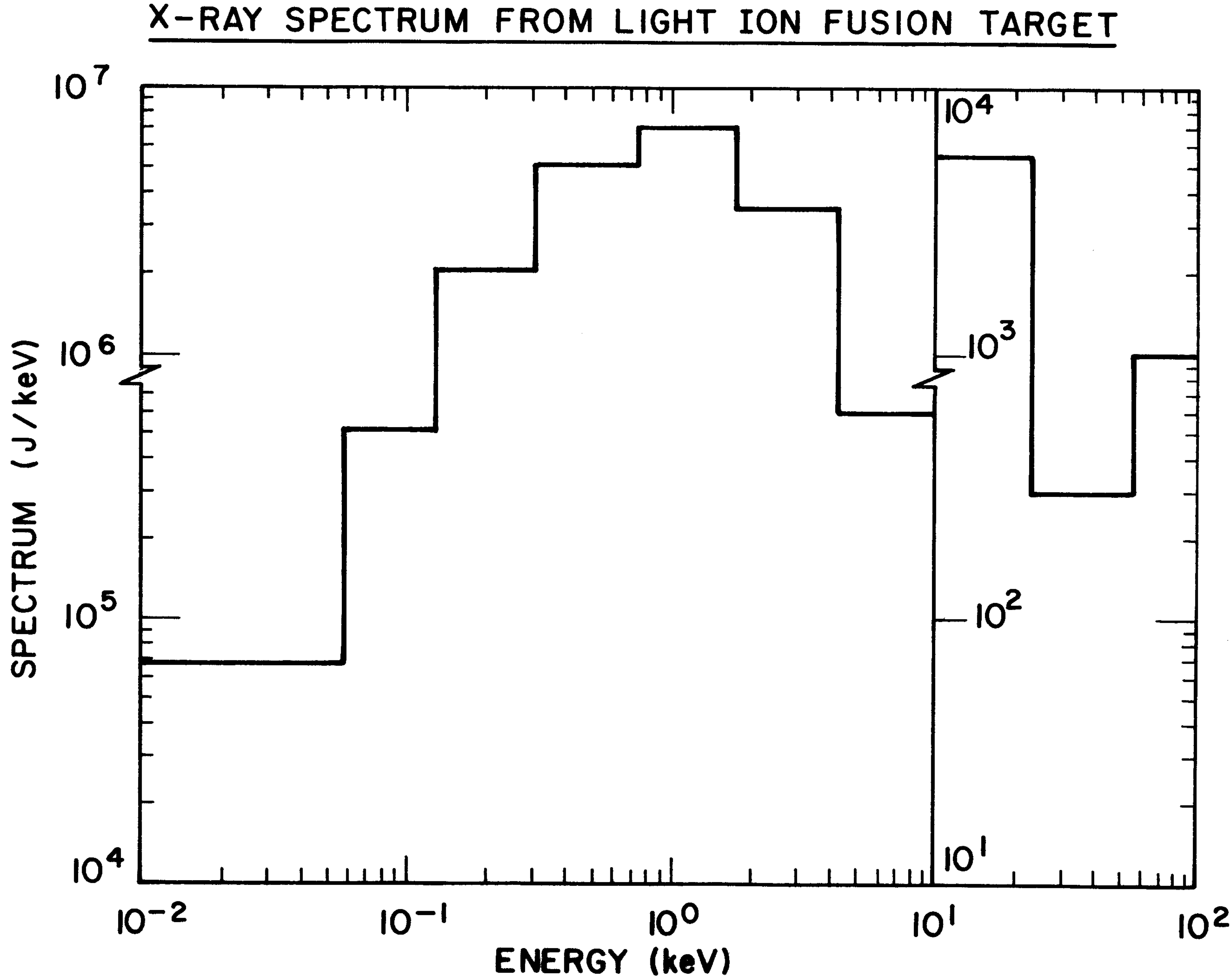


Figure 5 X-ray spectrum of light ion fusion target.

## III. Fireball Calculations

When the light ion beam fusion target explodes in a gas filled chamber the x-rays emitted by the target are attenuated by the gas. Likewise, the expanding ionic debris is stopped in the gas, creating a fireball. This fireball propagates to the first wall imparting an overpressure. The gas also reradiates a portion of the energy that it absorbs and this represents a thermal heat flux on the first wall. This thermal loading and overpressure will also affect any diagnostics that are located at the first wall. In this section we present results of calculations that estimate these quantities.

The fireball calculations were done using the MF-FIRE multifrequency radiation-gas dynamics computer code.(11) Some details about this code are given in Table 3. The physical properties of the gas were computed using the MIXERG multifrequency opacity and equation of state computer code.(12) Details about this code are given in Table 4. Using the MF-FIRE code we can calculate the prompt x-ray attenuation in the gas and the unattenuated x-rays reaching the first wall. The energy deposited by the attenuated x-rays gives an initial temperature distribution in the gas. The code also models the slowing down of the ions in the gas and uses this as an energy and momentum source term in the gas dynamics equations. For our target design we assumed that all of the ion energy was in the form of lead and neglected the other ionic species in the target. These calculations were done for two types of gases: argon and nitrogen. In both cases we assumed a pressure of 10 torr. This is believed to be the pressure required to support z-pinch plasma channel formation. In Table 5 we give specific parameters for four calculations. We calculated the energy fluence at two different positions for each of the two gases.

## Table 3. Details About MF-FIRE

1. One-dimensional lagrangian hydrodynamics.
2. One fluid equation of motion - artificial viscosity treatment.
3. Two temperature (plasma and radiation) heat flow.
4. Multifrequency radiative transfer option.
5. Flux limited diffusion approximation to energy flow.
6. Equations of state and multifrequency opacities in tables generated by MIXERG (see Table 4).
7. Target x-ray attenuation in gas and resultant temperature distribution.
8. Target ionic debris slowing down by the gas, with energy and momentum sources in the gas dynamics equations.

Table 4. Details About MIXERG

1. Semi-classical treatment of atomic physics.
2. Saha ionization and coronal ionization models.
3. Photon interaction processes include: photo-ionization, inverse bremsstrahlung, atomic transition line absorption, Thomson scattering, and absorption by plasma waves.
4. Two temperature Rosseland and Planck averaged opacities.
5. Multigroup Rosseland and Planck averaged opacities.
6. Average ionization state, specific internal energy, and heat capacity equation of state information.
7. Treats mixtures of up to five gases.
8. Creates machine readable tables of data.

Table 5. Specific Parameters for Fireball Calculations

| Parameter | Case 1 | Case 2 | Case 3 | Case 4 |
|---|---|---|---|---|
| • Cavity Radius (m) | 3 | 3 | 3 | 3 |
| • Distance from Target to Detector (m) | 3 | 1 | 3 | 1 |
| • Cavity Gas Type | Ar | Ar | $N_2$ | $N_2$ |
| • Cavity Gas Pressure at 0°C (torr) | 10 | 10 | 10 | 10 |
| • Cavity Gas Initial Temperature (eV) | 0.0925 | 0.0925 | 0.0925 | 0.0925 |
| • Cavity Gas Initial Density ($g/cm^3$) | $2.36 \times 10^{-5}$ | $2.36 \times 10^{-5}$ | $1.65 \times 10^{-5}$ | $1.65 \times 10^{-5}$ |
| • Cavity Gas Initial Number Density ($cm^{-3}$) | $3.55 \times 10^{17}$ | $3.55 \times 10^{17}$ | $7.1 \times 10^{17}$(*) | $7.1 \times 10^{17}$(*) |

---------------------

*Diatomic nitrogen must be modeled using twice the actual initial molecular number density.

In Fig. 6 we show the x-ray spectrum at 3 meters from the target in a chamber filled with 10 torr of argon. On this figure we also show the target x-ray spectrum at the surface of the target. We see that only 1.8 MJ of x-ray energy gets through the gas, out of a released energy of 22 MJ. (Note the change of vertical scale at E = 10 eV and E = 10 keV on this and the following figures.) At low photon energy, between 1 eV and 10 eV we record the spectrum of x-rays emitted by the hot argon fireball. This 14.4 MJ of soft x-rays represents a very severe surface heat loading on any component positioned at the first wall. In Fig. 7 we show the heat flux and overpressure at the first wall as a function of time. The maximum recorded overpressure is 0.16 MPa. Figure 8 is an R - t diagram showing the shock wave propagation to the first wall. The shock arrives at ~ 0.75 msec after the target explosion.

In Fig. 9 we show the same spectral information for a component placed at 1 meter from the target, within the 3 meter vessel. This is shown schematically in Fig. 1. Here again we plot the original target x-ray spectrum as well as the unattenuated spectrum at 1 meter from the target. In this case we get 6.2 MJ of unattenuated prompt x-rays. Also shown is the thermal x-ray spectrum which contains 17.9 MJ of energy.

In the third case we analyzed nitrogen gas. Figure 10 shows the same kind of spectral information as before. In the case of the lower-Z nitrogen, we get more energy in unattenauted x-rays (8.1 MJ) at the first wall. Once again the nitrogen, like the argon, filters out all of the x-rays below 1 keV. However, the nitrogen passes almost all of the x-rays above 4 keV. The nitrogen also releases less energy in the form of soft x-rays, in this case only 2.1 MJ as compared to 14.4 MJ for argon. However, the overpressure is nearly twice as large, 0.28 MPa, as the comparable argon case.

Figure 6  X-ray spectrum at 3 meters from the LIF target in a 3 m chamber filled with 10 torr Ar.

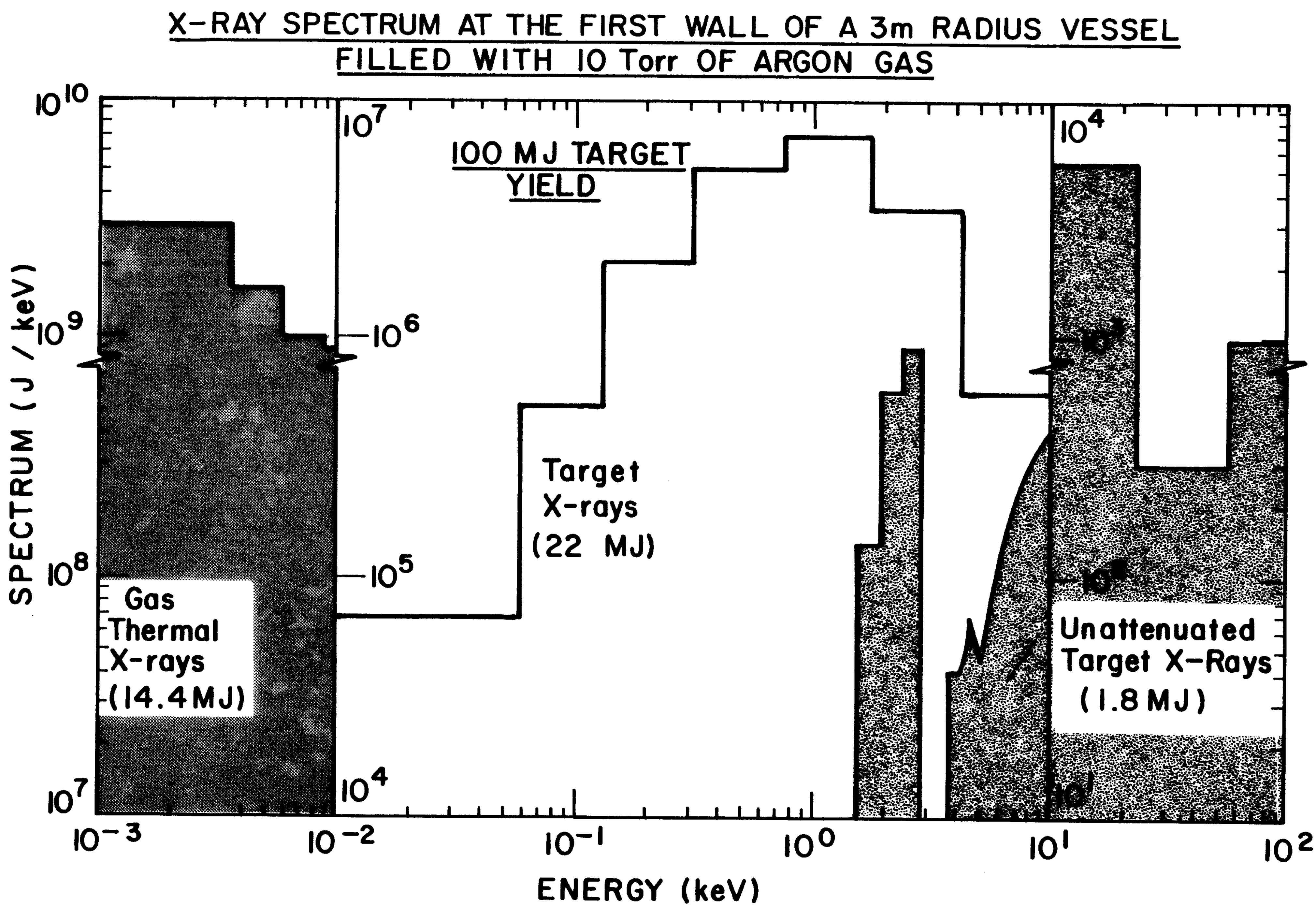

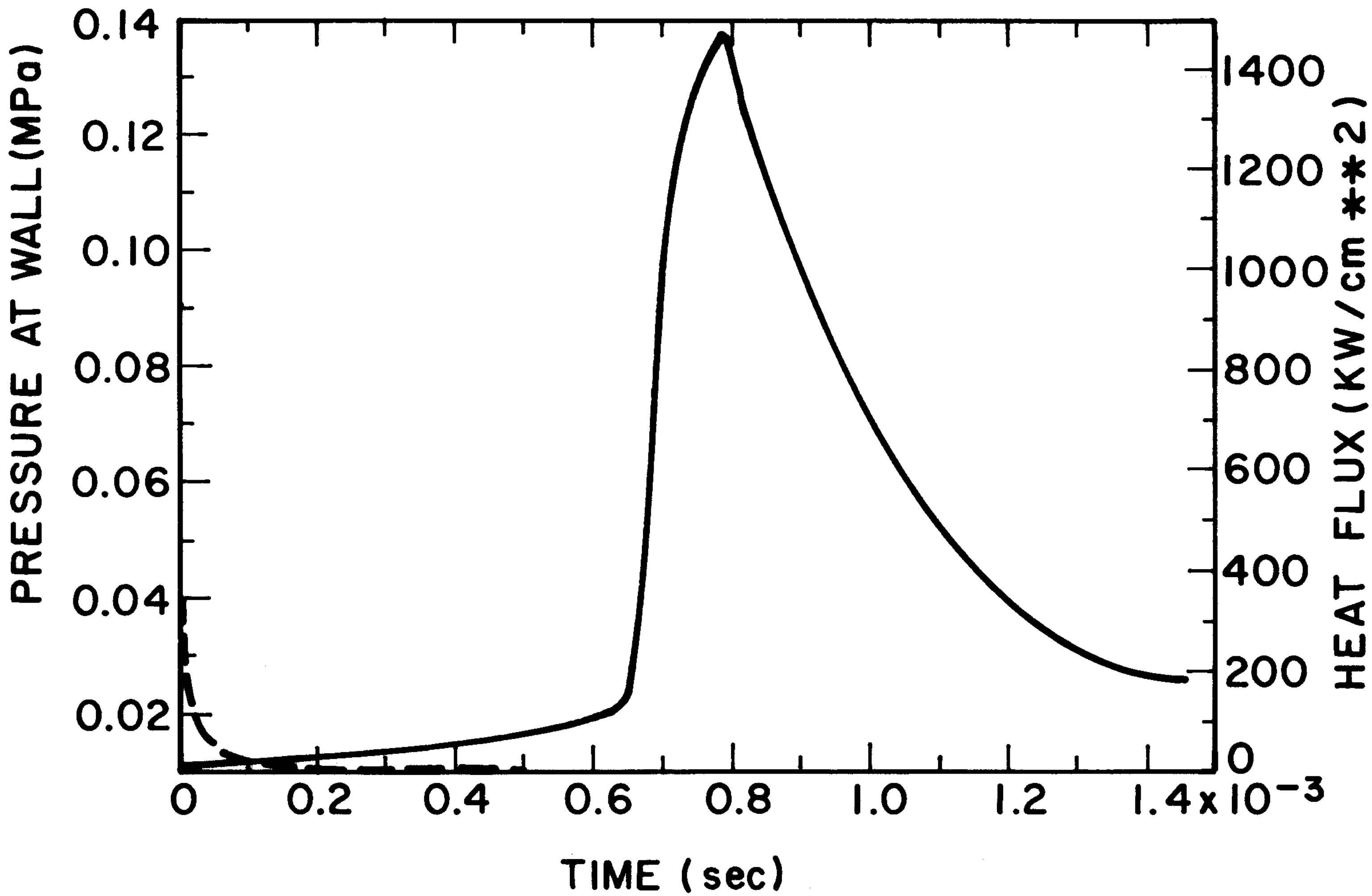


Figure 7 Heat flux and overpressure vs. time at the first wall in a 3 meter chamber filled with 10 torr of argon.

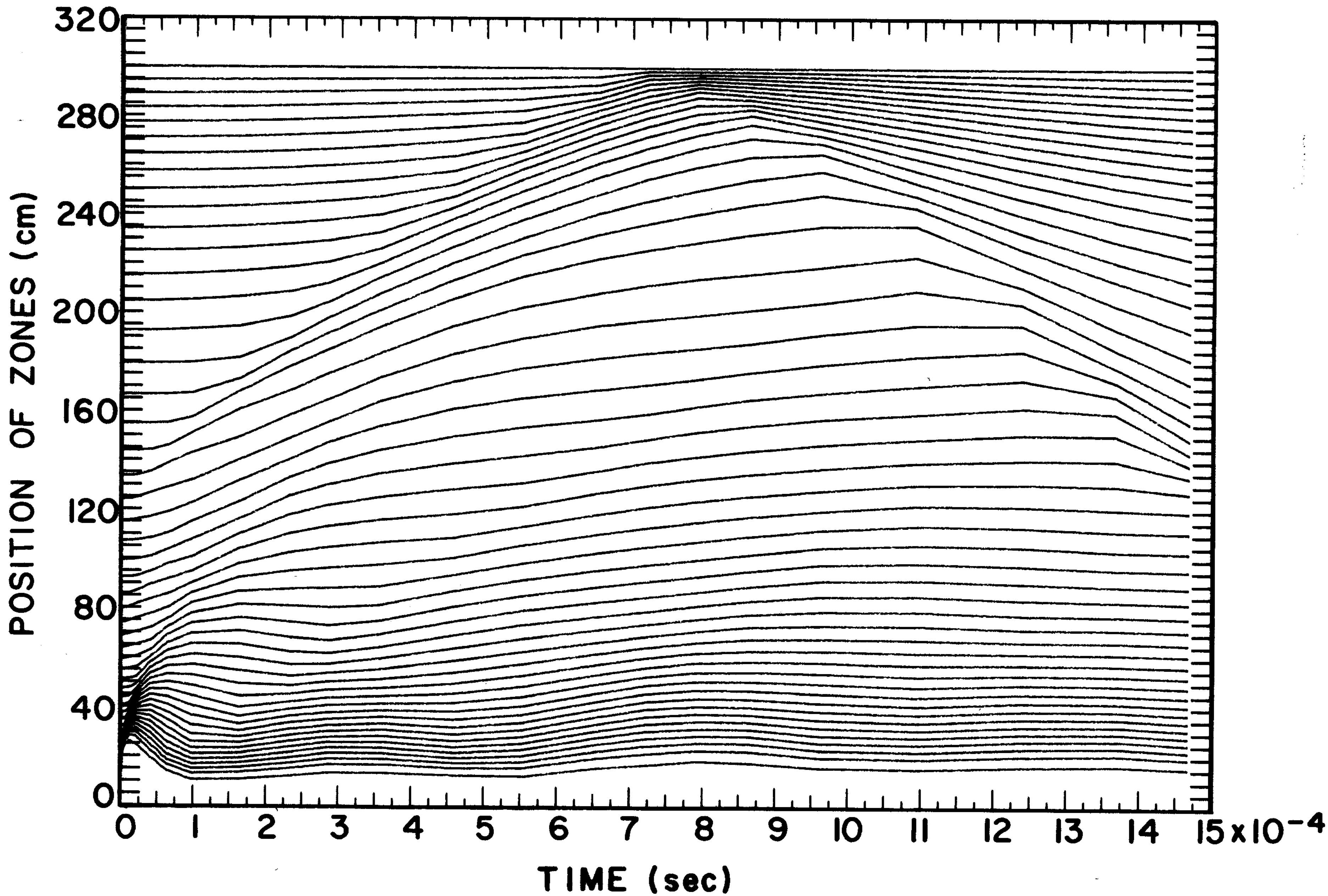


Figure 8. R - t diagram of the gas response for a 100 MJ target explosion in a 3 meter chamber filled with 10 torr of argon.

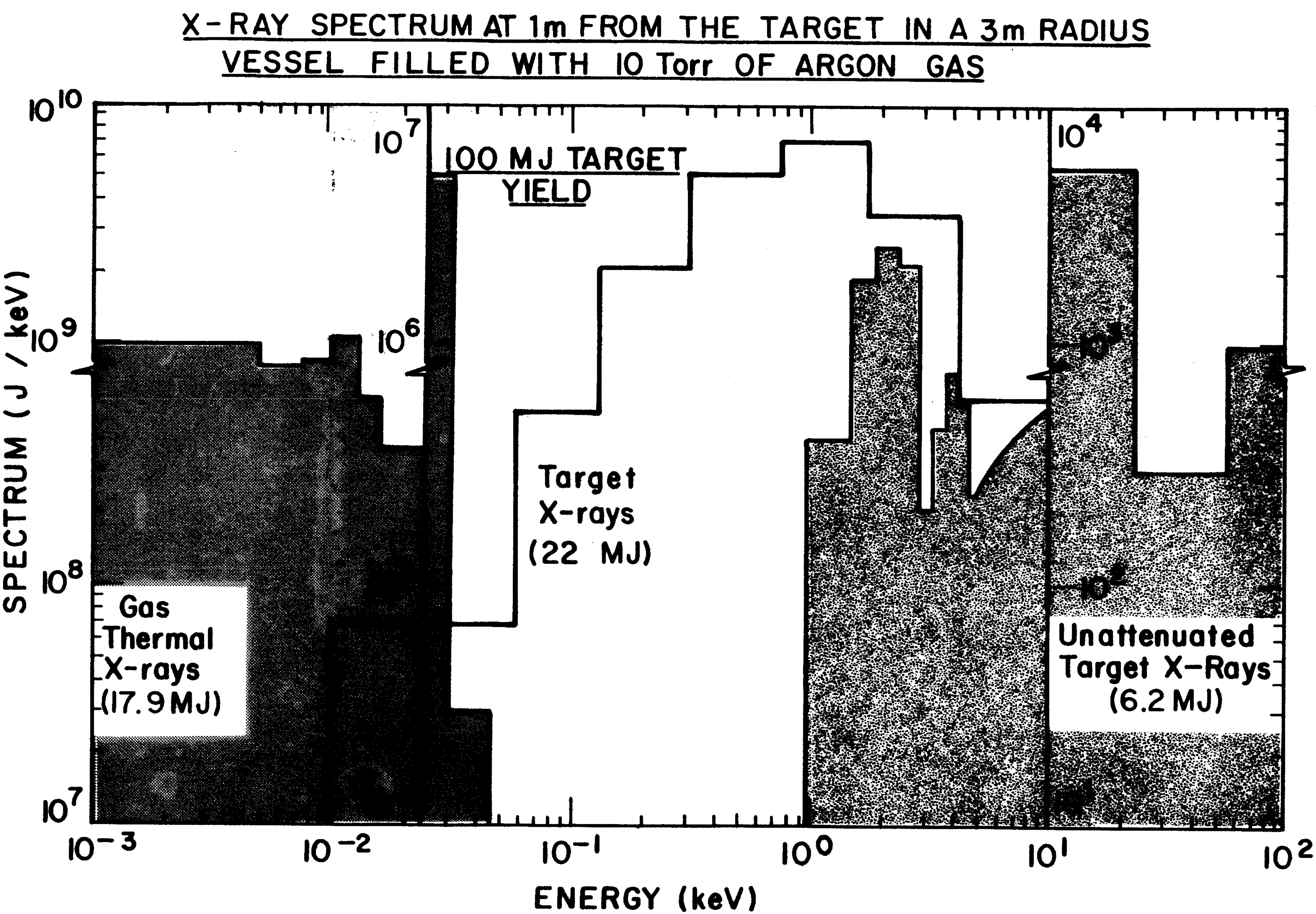


Figure 9. X-ray spectrum at 1 meter from the LIF target in a 3 meter chamber filled with 10 torr of argon.

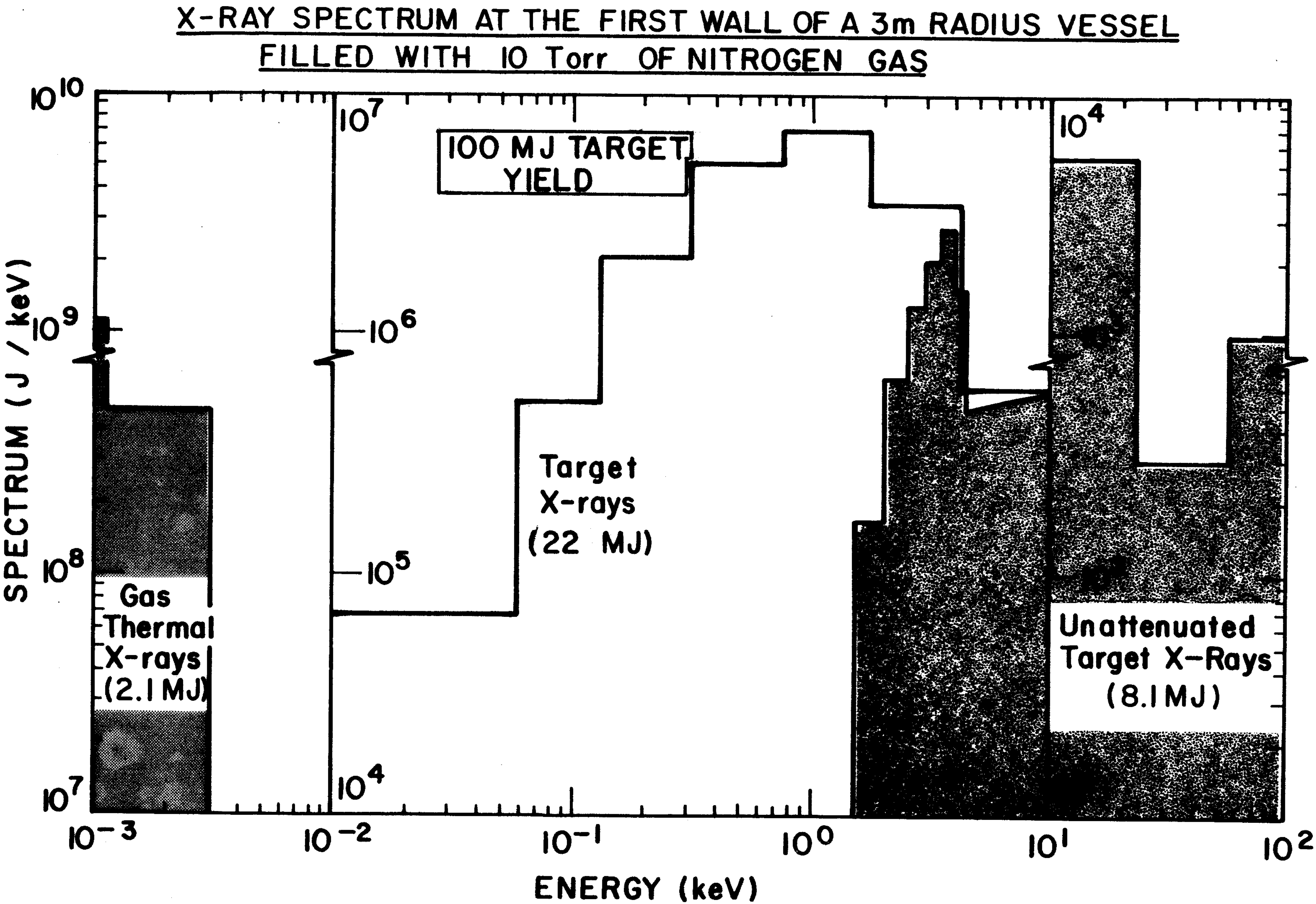


Figure 10. X-ray spectrum at 3 meters from the LIF target in a 3 meter chamber filled with 10 torr of nitrogen.

Finally, in the fourth case we calculate the x-ray spectrum on a surface located at 1 meter from the target in nitrogen gas. The results of this calculation are given in Fig. 11. Here we have 11.1 MJ in unattenuated prompt x-rays at energies greater than 1 keV and 4.5 MJ of soft thermal x-rays from the hot fireball. The overpressure is substantial -- 1.6 MPa.

The various fluences for these four calculations are summarized in Table 6. Also given are the neutron and gamma ray fluences. In all cases the energy fluence of the long range neutrons is much greater than any of the x-ray contributions. The prompt gamma ray signal is quite small in comparison to the x-rays. In general, the nitrogen transmits a greater fraction of the hard (> 1 keV) prompt x-rays than the argon. The argon produces a significantly higher soft x-ray fluence than the nitrogen.

## IV. Conclusions

These calculations demonstrate that nitrogen is a better choice for chamber gas if the surface heat load due to soft x-rays is to be minimized. However, nitrogen transmits a greater fraction of the more penetrating hard x-rays. On the other hand, argon attenuates more of the hard x-rays but also creates a high surface heat load.

If such a facility were to be used for studying the effects of hard x-rays, then these calculations demonstrate that a diagnostic package located at 1 meter from the target would receive a pulsed energy fluence of 88 J/cm$^2$ in x-rays with energies greater than 1 keV. However, the soft x-ray fluence of 36 J/cm$^2$ would vaporize the surface of the diagnostic package unless a sacrificial shield were placed in front of it. The use of low-Z shields such as plastic or Be will be investigated as part of an effort to design an in-situ diagnostic module for the TDF.

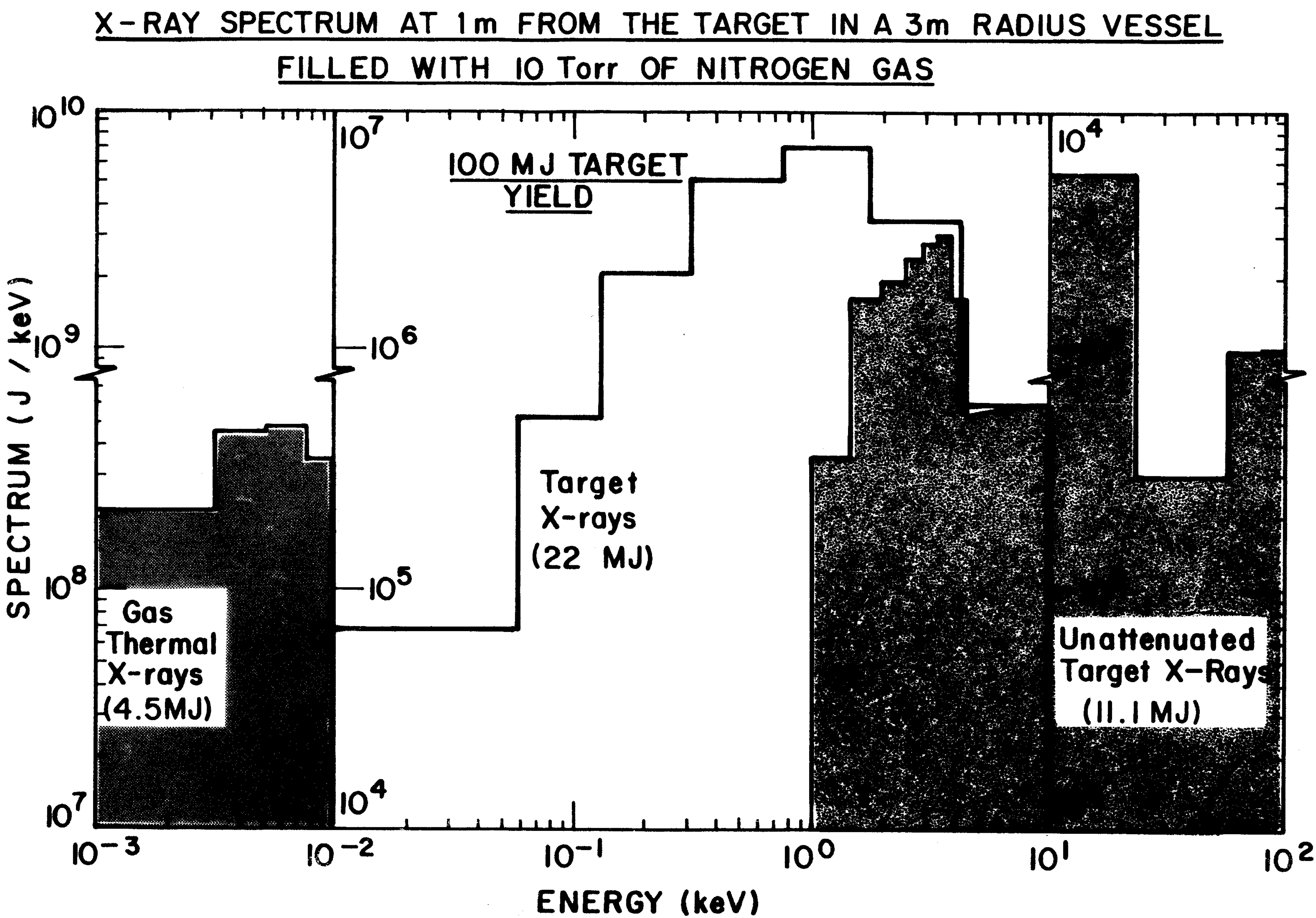


Figure 11. X-ray spectrum at 1 meter from the LIF target in a 3 meter chamber filled with 10 torr of nitrogen.

Table 6. Fluences on the Detector at 1 and 3 Meters for Argon and Nitrogen

| Gas Type | Distance from Target to Detector | Energy Density Hard X-Rays | Energy Density Soft X-Rays | Energy Density γ-Rays | Energy Density Neutrons | Max ΔP |
|---|---|---|---|---|---|---|
| | (cm) | ($J/cm^2$) | ($J/cm^2$) | ($J/cm^2$) | ($J/cm^2$) | MPa |
| Ar | 300 | 1.6 | 12.7 | 0.13 | 63.5 | 0.16 |
| Ar | 100 | 4.9 | 142. | 1.2 | 572. | 0.36 |
| $N_2$ | 300 | 7.2 | 1.8 | 0.13 | 63.5 | 0.28 |
| $N_2$ | 100 | 88. | 35.8 | 1.2 | 572. | 1.60 |

Acknowledgments

This work was supported by Sandia National Laboratory under contract no. DE-AS08-81DP40161.

References


1. D.L. Cook, "Preliminary Conceptual Design and Engineering Aspects of a Light Ion Fusion Target Development Facility (TDF)," Proc. of 9th Symp. on Engin. Probs. of Fusion Res., Chicago, IL, Oct. 1981, p. 664.

2. J.R. Freeman, L. Baker, and D.L. Cook, "Plasma Channels for Intense Light Ion Beam Reactors," Nucl. Fusion 22, 383 (1982).

3. G.A. Moses and R.R. Peterson, "First Wall Protection in Particle Beam Fusion Reactors," Nucl. Fusion 20, 849 (1980).

4. R.R. Peterson, G.W. Cooper, and G.A. Moses, "Cavity Gas Analysis for Light Ion Beam Fusion Reactors," Nucl. Tech./Fusion 1, 377 (1981).

5. R.R. Peterson, K.J. Lee, and G.A. Moses, "Low Density Cavity Gas Fireball Dynamics in the Light Ion Beam Fusion Target Development Facility," Proc. of 9th Symp. on Engin. Probs. of Fusion Res., Chicago, IL, Oct. 1981, p. 668.

6. R. Bangerter, Laser Program Annual Report - 1976, Lawrence Livermore Laboratory Report UCRL-50021-76, pp. 4-44.

7. B. Badger et al., "HIBALL - A Conceptual Heavy Ion Beam Driven Fusion Reactor Study," University of Wisconsin Fusion Engineering Program Report UWFDM-450, June 1981, p. III.1-1.

8. G.A. Moses, G.R. Magelssen, R. Israel, T. Spindler, "PHD-IV, A Plasma Hydrodynamics, Thermonuclear Burn, Radiative Transfer Computer Code," University of Wisconsin Fusion Engineering Program Report UWFDM-194 (revised January 1982).

9. RSIC Code Package CCC-254, "ANISN-ORNL," Radiation Shielding Information Center, Oak Ridge National Laboratory, Oak Ridge, TN.

10. M.E. Sawan, G.A. Moses, and G.L. Kulcinski, "Time Dependent Neutronics Analysis for the HIBALL Heavy Ion Beam Fusion Reactor," Nucl. Tech./Fusion 2, 215 (1982).

11. G.A. Moses, T.J. McCarville, and R.R. Peterson, "Documentation for MF-FIRE, A Multifrequency Radiative Transfer Version of FIRE," University of Wisconsin Fusion Engineering Program Report UWFDM-458, March 1982.

12. R.R. Peterson and G.A. Moses, "MIXERG, An Equation of State and Opacity Computer Code," to be published in Computer Physics Communications. Also, University of Wisconsin Fusion Engineering Program Report UWFDM-464, March 1982.